DAMAGE DETECTION IN BUILT-UP COMPOSITE STRUCTURES USING LAMB WAVE METHODS

Seth S. Kessler* and S. Mark Spearing

Department of Aeronautics and Astronautics, Massachusetts Institute of Technology, Cambridge, MA 02139, USA

* Corresponding author: *Email address* - sskess@mit.edu Phone – 617-253-8907 *Fax* - 630-214-8749

ABSTRACT

Cost-effective and reliable damage detection is critical for the utilization of composite materials. This paper presents part of an experimental and analytical survey of candidate methods for in-situ damage detection of composite materials. Results are presented for the application of Lamb wave techniques to quasi-isotropic graphite/epoxy finite element and test specimens containing representative damage modes, including delamination, transverse ply cracks and through-holes. Optimal actuator and sensor configurations were developed from the Lamb wave equations, along with appropriate driving parameters. A previous paper reported the results of linear wave scans performed on narrow laminated specimen and sandwich beams with various cores by monitoring the transmitted waves with piezoceramic sensors (PZT). The current work has focused on built-up structures, such as stiffened composite plates and a composite sandwich cylinder. This method has also been applied to 2-D plates during the present work. Lamb wave techniques have been proven to provide more information about damage type, severity and location than previously tested methods (frequency response techniques), and may prove suitable for structural health monitoring applications since they travel long distances and can be applied with conformable piezoelectric actuators and sensors that require little power.

Keywords: Polymer-matrix composites; Damage detection; Structural Health Monitoring; Lamb waves;

1. INTRODUCTION

Structural Health Monitoring (SHM) has been defined in the literature as the "acquisition, validation and analysis of technical data to facilitate life-cycle management decisions." [1] More generally, SHM denotes a system with the ability to detect and interpret adverse "changes" in a structure in order to improve reliability and reduce life-cycle costs. The greatest challenge in designing a SHM system is knowing what "changes" to look for and how to identify them. The characteristics of damage in a particular structure plays a key role in defining the architecture of the required SHM system. The resulting "changes," or damage signature, will dictate the type of sensors that are required, which in-turn determines the requirements for the rest of the components in the system. The present research project focuses on the relationship between various sensors and their ability to detect "changes" in a structure's behavior. Previous papers have focused on the application of modal analysis and Lamb wave techniques to narrow laminated coupons [2-6]. Modal analysis techniques have shown good sensitivity to the presence of damage, however not much information about the damage type of location can be determined by this inherently global method. Lamb wave methods have recently re-emerged as a reliable way to locate damage in these materials [7-9]. Various techniques have been implemented in the literature, which have been presented in previous papers. The most complete work in this field can perhaps be found in Valdez's PhD thesis [10]. During the course of his work he performed many experiments on quasi-isotropic graphite/epoxy composite specimens, pulsing them with Lamb waves in various configurations to detect delaminations. He also simulated the propagation of Lamb waves in plates using a finite element code. Much of the research presented in this paper follows Valdez's work, extending it to various other types of damage, to built-up structures, and an attempt to optimize the testing parameters.

2. LAMB WAVE PROPAGATION PARAMETERS

Lamb waves are a form of elastic perturbation that can propagate in a solid plate with free boundaries [11, 12]. This type of wave phenomenon was first described in theory by Horace Lamb in 1917, however he never attempted to produce them [13]. The present work utilizes PZT piezoelectric patches to excite the first anti-symmetric Lamb wave (A0 mode). This wave was chosen since it can propagate long distances with little dispersion, and no higher modes are present to clutter the resulting response waves [10]. There is currently no standard or even a best-practice precedent for damage detection via Lamb wave testing. Several procedures have been developed in the literature, each with valuable characteristics, and each with some degree of arbitrariness. A

major goal of the present research was to optimize the parameters used to propagate the Lamb waves based upon the various equations that describe their motion. In previous Lamb wave papers, a detailed derivation has been presented for the Lamb wave solutions to the wave equation, and the effects various variables had on the sensitivity of these methods to damage was discussed. The present work places these findings into selection guidelines to choose the appropriate actuating frequency, pulse shape, and sensor geometry for a particular Lamb wave application. Also discussed in the following sections are the topics of sensor spacing and data interpretation. All of these guidelines were used to define the testing parameters for the experimental procedures that followed. This set of tools could be used in parallel by an engineer developing a SHM system for a vehicle to decide if the Lamb wave method would provide satisfying results for their application, and to determine the appropriate driving parameters to obtain the best damage detection resolution.

2.1 Frequency Selection

The first step in defining an appropriate Lamb wave damage detection solution is to select an appropriate driving frequency. This procedure commences by finding the Lamb solution for the wave equation, and plotting the dispersion curves for each section to be monitored. By entering the stiffness and density properties for a particular material, the resulting dispersion curves provide a range of potential wave velocities for the A_0 (first anti-symmetric) mode driven at different frequency-thickness products. For a given thickness, ideally one would like to choose the least dispersive driving frequency for the Lamb wave being generated, which generally exists where the slope of the phase velocity curve is equal to zero. This is because at low frequencies, the dispersion curves have steep slopes and thus are very sensitive to small variations in frequency making it difficult to maintain a constant velocity to predict the time of flight. The A_0 mode, however, follows a square root relationship with frequency until higher values, thus the operating frequency needs to be chosen by a different criteria. The higher the frequency the smaller the slope of the A_0 dispersion curve, although at a certain point other higher order Lamb waves begin to exist simultaneously and the signal becomes cluttered. The wave velocities are also much faster at higher frequencies, increasing data acquisition requirements.

To balance these issues, the following procedure should be followed. First plot the dispersion curves for the material, and locate the frequencies at which the Rayleigh velocity is obtained and where the A_1 mode begins to be excited. If the Rayleigh velocity is below the point where the next anti-symmetric mode is generated (which

normally is not true) then this is the critical frequency; otherwise it would be wise to choose a point about 10% below the A_1 origin point as the critical frequency. Next, it must be determined if the data acquisition capabilities are able to capture a wave traveling at this velocity. Typically, the data acquisition rate should be 10 times the frequency of the signal it is sampling, so the selected driving frequency may have to be lowered if the sampling rate is unobtainable. Also, with knowledge of the effects of various damage types on the stiffness of a particular material, the resolution of change for the resultant signal, or "observeability," can be predicted in order to determine the detection limitations with respect to flaw size for a given data acquisition capability. It would also be prudent to check on the actuator capabilities to generate that range of frequencies. A final consideration to fine tune the driving frequency is to calculate the natural frequencies of the structure to be monitored, either analytically or by finite element models, and to select a driving frequency that coincides with a normal mode in the desired frequency range. The natural frequencies of the structure play a small role in the amplification or attenuation of the transmitted wave, whereas the wave can travel with less disturbance at a resonant frequency.

Using this procedure, an effective experimental test procedure was determined for the present research. The material constants in the propagation direction for the composite laminates to be analyzed were calculated by classical laminated plate theory, and then entered into the Lamb wave model. For the narrow coupon tests, 15 kHz was selected as an optimal frequency, 50 kHz for the sandwich beam tests, and 40 kHz for the micro-satellite bus structure (all to be described further in the experimental procedures section). These frequencies were obtained from their slope and location on the dispersion curves, evidence from previous research suggesting these frequencies for specimens of similar geometries, and brief experimentation using a function generator to verify the maximum response amplitude for the range of driving frequencies. Following this procedure it was determined that graphite/epoxy composite materials were a good candidate for Lamb wave methods, and that with the detection capabilities of the data acquisition system that a reasonable change in stiffness (5-10%) could be resolved.

2.2 Pulse Shape Selection

The second set of variables explored was the actuation pulse parameters. These included the pulse shape, amplitude and number of cycles to be sent during each pulse period. These parameters were varied analytically and verified experimentally on a control specimen to observe their effect on the Lamb waves generated. First, several candidate signal shapes were compared in Matlab™ by using their power-spectral-density (PSD) plots. Similarly

the effect of the number of cycles per period for the different shaped signals was observed in the PSD plots by comparing the energy dedicated to the principal driving frequency. The more energy dedicated to the desired driving frequency, the stronger the Lamb wave and the more accurate the wavespeed calculation, and hence the more sensitive and reliable the damage detection capability. Of the signal shapes that were analyzed and experimented, pure sinusoidal shapes appear to excite Lamb wave harmonics the most efficiently, since they are periodic, smooth and have comparatively quick rise times to their peak amplitude as compared to a parabolic shape. A Hanning window helps to narrow the bandwidth further to focus the maximum amount of energy into the desired actuating frequency with the least "spill-over" from neighboring frequencies. For the present research, a signal of 3.5 sine waves under a Hanning window was used.

Once the driving frequency and signal shape have been selected, there is then a trade between the number of waves that can be sent in an actuating pulse and the distance from abrupt features in the structure. The number of cycles of a periodic function desired to actuate the piezoelectric actuator is one of the more complicated decisions to be made for Lamb wave techniques. The fast Fourier transform (FFT) of a continuous sine wave would yield a single peak at the driving frequency, however for a few finite cycles, the FFT appears as a Gaussian curve with a peak at the driving frequency. Thus, the more waves sent into a driving pulse, the narrower the bandwidth and the less dispersion. The problem in a short specimen though, is the more waves in the pulse, the less time between the last signal sent and the first returning reflected signal, so the response is more difficult to interpret. An appropriate number of cycles can be determined by the maximum number of waves that can be sent in the time it takes for the lead wave to travel to the sensing PZT patch. It is also convenient to use intervals of half cycles so that the sent sinusoidal pulse becomes symmetric. Research from the literature has used signals varying from 3.5 to 13.5 cycles per actuating pulse [7-10]. Since the specimens in the current research are relatively short, few cycles could be actuated without disturbing the received signal; thus 3.5 cycles were used to drive the piezoceramic actuators. Lastly, by increasing the driving voltage the magnitude of the strain produced by the propagating Lamb wave proportionately increases. In these experiments, driving with 5-10V produced a 10-25 mV response due to the wave sensed by the PZT patch. Increasing the amplitude also increases the signal to noise ratio to yield a clearer signal, since the static noise received by the PZT patch is usually in the 1-5 mV range. Also, a SHM system should be as low power as possible, thus the voltage should be chosen to be the minimum required to resolve the desired damage size. The optimal driving voltage was therefore chosen to be 5V peak-to-peak for these experiments.

2.3 Actuator Dimensions

PZT piezoceramic actuators were chosen for the present research due to their high force output at relatively low voltages, and their good response qualities at low frequencies. The generic shape of the actuator should be chosen based upon desired propagation or reception directions. Several researchers in various fields have examined the effects of piezoelectric wafer dimensions on the efficiency of their actuation [14, 15]. Waves propagated parallel to each edge of the actuator, i.e. longitudinally and transversely for a rectangular patch and circumferentially from a circular actuator. The width of the actuator in the propagation direction is not critical, however the wider it is, the more uniform the waveform created. As cited in the literature though, there is an important sinusoidal relationship between actuating frequency and actuator length [11]. In the direction of propagation the desired actuator length 2a for most efficient signal is:

$$2a = l\left(n+\frac{1}{2}\right) = \frac{c_p}{f}\left(n+\frac{1}{2}\right) \quad \text{for } n = 0, 1, 2, 3... \tag{1}$$

This value of 2a could either be a rectangular side length or the diameter of a circular actuator. This equation could also be used to determine actuator minimum dimensions, in order to inhibit waves from propagating in undesired directions. For the experimental procedures in the present research, PZT actuators of 1.5 cm x 0.75 cm were selected based upon this equation.

2.4 Sensor Spacing

Two important concepts to understand in wave propagation are dispersion and attenuation. Dispersion is the change in wavespeed in a material with respect to frequency, which was demonstrated graphically in the previous section. Since the group velocity is related to the rate of change of the phase velocity at a given frequency, the phase and group velocities are the same for a non-dispersive material. Attenuation is the change in amplitude of a traveling wave over a given distance. While propagating through a solid medium, energy is transferred back and forth between kinetic and elastic potential energy; when this transfer is not perfect, attenuation occurs. This loss in energy can be due to heat being generated, waves leaking into sideband frequencies or spreading into different propagation paths, restraints such as a bonded core, or in the case of composite materials, the fibers can provide reflecting surfaces, which would deteriorate the transmitted wave strength. These two concepts influence each other

as well, as increased dispersion causes higher attenuation, and vice-versa. A mathematical approximation to this correlation from the literature that relates the attenuation as a function of propagation distance is:

$$A = \frac{1}{KL} \rightarrow \frac{1}{\sqrt{K_r L}} \tag{2}$$

where A is the attenuation factor and L is the propagation distance. The attenuation tends to the slower Rayleigh attenuation value as the specimen becomes thicker [11]. An example of this relationship can be seen in the symmetric Lamb wave modes that tend to not travel as far as the anti-symmetric ones, which can be attributed to their dispersive nature (it is difficult to keep the two surfaces of the medium in phase with each other, which causes a high rate of phase velocity change). It has also been experimentally determined that fluids on the surface of a solid can affect the attenuation of the wave, however this effect is limited mostly to the symmetric modes so will not be discussed in detail in this paper [12]. Analytical studies have also been performed to formulate the change in dispersion (and hence attenuation) in curved panels [11]. It was found that the phase velocity is changed by the relationship:

$$\overline{c}_p = \left(1 + \frac{c_p^2}{w^2 R^2}\right) c_p \tag{3}$$

where c_p is the original phase velocity and R is the radius of curvature. When the phase velocity dispersion curve is adjusted by this formula, the slight increase in dispersion is readily apparent. Using these two relationships, an approximation can be made to determine the appropriate spacing between the actuators and sensors on a structure. The design objective of a SHM system is to achieve the most structural coverage with the least number of sensors, thus the optimal sensor spacing must be calculated. Using **Equation 2**, which specified an inversely proportional relationship between propagation distance and signal amplitude that was also dependant on the wave number, an acceptable signal loss can be specified for the voltage sensitivity of a data acquisition system. For the present research this was determined to be 25%, and from this percentage an estimated actuator-sensor spacing was be calculated to be 0.5m.

2.5 Signal Interpretation

The key to reliable and high-resolution damage detection is good signal interpretation. Perhaps the most important factor that has allowed Lamb wave techniques to flourish recently is the development of wavelet analysis. Wavelet decomposition is analogous to the Fourier decomposition, however instead of just using sines and cosines,

complex “mother wavelets” are used to break down the signal [16]. The idea for the wavelet decomposition was first presented by Haar in 1910, however the square wave he used was not very practical for most applications. It was not until 1988 when Daubechies introduced a fractal-like mother wavelet, was the full potential of wavelet analysis for signal decomposition and compression realized. The mother wavelet is essentially used as an orthogonal basis vector to filter the signal, and is scaled and shifted to approximate the frequency components of the signal. The virgin signals taken from the sensors were in the form of a time history of small voltages caused by strains induced by the impinging Lamb waves. These measurements were then passed to Matlab™, where the Morlet wavelet was used to decompose the signals, since its shape was closest to the driving pulse shape, which makes the processing more accurate and efficient [17]. To analyze the measurements, the Morlet wavelet was scaled between 0 Hz and twice the driving frequency and it was subsequently shifted through the entire time axis. The results of this analysis could be visualized in two forms. The first was a waterfall plot, which plots all the frequency scales versus time, representing the energy present at a point by color-coded intensity. Secondly, each of these scale bands could be plotted independently to allow observation of the numerical amplitude of signal energy versus time. Using the second method, by looking at the central scale band one could filter out all frequencies other than the central driving frequency from the received signals. This provides a clear, filtered view of the transmitted energy from the actuator to the sensors over time for an accurate time of flight measurement. Then, by looking at the waterfall plot, one could potentially gain insight into the damage in the specimen from the intensities of energy that have been shed into sideband frequencies. The experimental results presented later in the present research were created using this procedure.

3. EXPERIMENTAL PROCEDURE

3.1 Narrow Coupon and Sandwich Beam Tests

The experimental procedures for the present research followed a building block approach [18], and the first set of experiments conducted on narrow composite coupons was presented in a previous paper. The laminates were 25 x 5 cm rectangular $[90/\pm45/0]_s$ quasi-isotropic laminates of the AS4/3501-6 graphite/epoxy system with various forms of damage introduced to them, including matrix-cracks, delaminations and through-holes. PZT piezoceramic patches were affixed to each specimen using 3M ThermoBond™ thermoplastic tape. Both the actuation and the data

acquisition were performed using a portable NI-Daqpad™ 6070E data acquisition board, and a laptop running Labview™ as a virtual controller. A single pulse of the optimal signal found in the previous section was sent to the driving PZT at 15 kHz to stimulate an A_0 mode Lamb wave, and concurrently the strain-induced voltage outputs of the other two patches were recorded for 1 ms to monitor the wave propagation. By plotting the magnitude of the wavelet coefficient at the peak driving frequency, the energy remaining from the input signal could be compared [16]. This procedure was also carried out for beam specimens with four different cores: low and high density (referred to as LD and HD) aluminum honeycomb, Nomex™, and Rohacell™, with a driving frequency of 50 kHz for these tests.

3.2 Stiffened Plate Tests

The next set of experiments examined damage detection in more complex stiffened specimens using Lamb waves. Laminated plates were manufactured similarly to the ones from the previous sections, however these specimens included a secondary cure in which ribs were bonded across the center of the plate using Cytec™ FM-123 film adhesive. Three different configurations of ribs were tested during this section of research. The first had a thin 2.5 cm wide aluminum C-channel rib with 1.2 cm tall webs, which was adhered to the laminate with the flat side facing down and the channel parallel to the sensors. The second configuration used two scrap pieces of the same composite laminate, one 2.5 cm wide the other 1.2 cm wide, which were bonded with FM-123 in a pyramid-like stack in the center of the laminate, again parallel to the sensors [18]. The final configuration was identical to the second one, except it had a 2.5 cm square Teflon strip inserted between the stiffening rib and the composite to create an artificial delamination in the center of the rib. For each of the configurations, actuating and sensing PZT sensors were affixed to opposite sides of the rib on the edges of the laminate in three locations—one pair that was centered on the laminate and one pair on either side of the centerline spaced 7.5 cm away. The purpose of these experiments was first to examine how the rib would effect the propagation of the Lamb waves, then to compare the propagation through ribs of various stiffness, and lastly to ascertain the feasibility of locating a delaminated region under a rib by comparing the received signal with undamaged regions. The test setup and data analysis procedure for the stiffened panel experiments were identical to that of the thin specimens with a driving frequency of 15 kHz.

3.3 Composite Sandwich Cylinder Test

The next level of complexity involved examining a relatively large built-up structure, a cylinder with a 40 cm diameter and length of 120 cm, which was constructed during previous research as a composite micro-satellite structure [19]. The two facesheets of the sandwich structure were manufactured from the same composite material as the other tested specimens and were of similar layup, and a 2.5 cm thick low-density aluminum honeycomb was bonded between them. An identical setup to that used on the other specimens was used on this cylinder to determine the feasibility of detecting known damaged regions in a large curved built-up structure. First, in a control region with no visual damage, an actuating piezo was placed on one end of the cylinder, and then sensing piezoceramic patches were placed down the length of the cylinder every 10 cm for 60 cm. These tests would not only provide a controlled time of flight for the structure, but would also provide data for the attenuation of the wave in a representative structure. Next piezo sensors were placed every 10 cm circumferentially over a 30 cm span to examine the attenuation of the Lamb wave signal in a curved section. Lastly, piezo sensors were adhered in positions 10 cm away longitudinally and at 5 cm increments circumferentially to attempt to quantify how far away from the main propagation channel the sensors could be placed to still sense a reliable measurement. Once again, the data analysis procedure for these experiments were identical to that of all the others, with a driving frequency of 40 kHz in this case because of the honeycomb core and slightly different layup.

3.4 2-D Plate Tests

The final test performed in pulse-transmission mode was to scan 2D laminated plates for damage. Graphite/epoxy panels measuring 30 x 30 cm were manufactured similarly to those of the previous experiments, but were not milled into smaller specimen for these experiments. Square PZT sensors measuring 1.5 cm on each side were affixed along the perimeter of the laminate, in the center of each side. The driving pulse was sent to actuate each PZT piece one at a time at 15 kHz, and simultaneously readings of resulting strains were measured from each of the other three patches; this would occur four times, each time actuating a different piezo. These results were also decomposed using the Morlet wavelet.

3.5 Self-Sensing Actuator Tests

As an alternative to pulse-transmission, some preliminary testing was also performed for the pulse-reflection of Lamb waves. Theoretically, this method should provide more information about damage location, since the time of flight of damage from reflection sites would be recorded so a triangulation could be performed. The setup for these tests was identical to the configuration from the 2-D plate tests, with PZT sensors placed in the center of each side. The only difference for these tests was that each PZT piece would serve as both a sensor and receiver simultaneously, collecting the reflected as well as the transmitted strain data for each pulse actuation. This "self-sensing" capability was achieved by using a full bridge circuit, represented in **Figure 1**, which was developed in the literature and adapted for use in these experiments. This circuit design would allow the data acquisition equipment to monitor the 10 mV strain measurements from the PZT without being overwhelmed by the 5 V driving signal [20].

4. ANALYTICAL PROCEDURE

Finite element models were created in ABAQUS™ to observe the small changes in time of flight caused by discontinuities in geometry or material properties. Models were built to represent each of the experiments that were performed, including narrow coupons, sandwich beams, 2-D plates with and without stiffening ribs, and finally a tube structure with sandwich construction. Each of these models were constructed identically to those described in a previous paper written on frequency response methods, using 1 cm^2 square shell elements, where the actuators were simulated by a coupled nodal moment. Again regions of cracked matrix were modeled as a local loss in stiffness, and delaminations were modeled by two half laminates with coincident unconnected nodes. Once processed, the time-steps were visualized as a movie file to measure the time of flight of the Lamb waves across the specimens, and to record visual evidence of dispersion and attenuation. By comparing the times of flight in these models, it was possible to determine the required distance between the piezoceramic actuator and sensors necessary to resolve the difference between waves traveling in a control versus a damaged specimen.

5. RESULTS

5.1 Experimental Testing Results

There were two sets of results obtained for both the thin coupons and the narrow sandwich beams. The first set of results included the virgin time traces of voltage from the PZT sensor at the far end of the specimen. The time traces for one of each type of specimen along with a superimposed control specimen are shown in **Figure 2**, and **Table 1** summarizes the estimated time of flight for each of the specimen based upon the plots. The second set of results for each specimen group was the outcome of the wavelet decomposition. Finally, **Figure 3** displays the wavelet coefficient results for the "blind test," comparing the two high density aluminum core control specimens with one known and one unknown damaged specimen.

Similar results were found for the built-up composite structures. The wavelet plots for each of the stiffened plate tests can seen in **Figure 4**. As described in the experimental procedure section, several sensors were placed along the composite sandwich cylinder at regular intervals. The wavelet plots for the axial propagation of the Lamb waves can be seen in **Figure 5**. Similar plots for the sensors along the path of the delaminated region are seen in **Figure 6**. The last sets of results are for the 2-D plate specimen. The wavelet plots for each of the four independent tests actuating with different piezoceramics can be seen in **Figure 7**. The time trace for the single "self-sensing" test performed at 45 kHz proved the feasibility of an actuator being used as a sensor as well, by sensing a wavefront with twice the time of flight as a sensor on the opposite side of the specimen. The reflected signal was quite small however, and more work would need to be performed to use this kind of sensor in future tests.

5.2 Analytical Results

The finite element models created in ABAQUS™ simulated the behavior of the Lamb waves as they traveled across the thin-shelled laminate. The products of these analyses were movie files that animated the vertical displacement of the nodes over time as the Lamb waves propagated from the loaded nodes. A series of still shots of a Lamb wave propagating in a control model can be seen in **Figure 8** and for a delaminated model in **Figure 9**. A summary comparing the recorded times of flight for each of the models that were analyzed can be found in **Table 2**. The FE results did not show much of a change between the control and cracked models for time of flight, however there was a noticeable reflected wave traveling from the cracked region after the Lamb wave had passed over it. The model with the through-hole exhibited a slight change in time of flight, and a small reflected wave was

observed as well. For both delamination models there was a significant increase in the time of flight due to the damaged region, as well as the introduction of a reflected wave with almost half the amplitude of the traveling wave. Additionally, the model with the asymmetric delamination created two wave fronts traveling at different speeds, which began to interfere with each other as they continued down the laminate. These FE results appear to be consistent with the experimental results, as will be further discussed in the following section.

Comparable results were found for each of the sandwich beam models, control and stiffened plate models and curved sandwich panel models. The time of flight measured for each of these models is documented in **Table 3**. Perhaps the most interesting results were discovered for the stiffened plate models. First, **Figure 10** displays the Lamb wave as it propagated across a plate with no stiffener attached as a controlled reference. Next, as seen in the series of stills for the plate with bonded composite stiffeners in **Figure 11**, as the wave traveled radially from the actuation region and reached the stiffened region, a uniform reflected wave began to propagate back towards the actuator, while the forward moving wave continued towards the opposite side, briefly speeding up in the stiffened region and shrinking in amplitude. For the stiffener with a delaminated region, seen in **Figure 12**, when the Lamb wave reached the stiffener it continued at the same speed and amplitude through the delaminated region while changing speed and displacement amplitude in the non-delaminated region. Perhaps the fascinating result was that the delaminated "slot" caused a fringe pattern to appear in both the continuing and reflecting waves, which there were regions of maximum and minimum displacement amplitudes radiating in constant angle intervals from the front of the delaminated area. The effect of a delaminated region in a curved sandwich panel was similar, where a very small amplitude wave propagated across the thick panel and was significantly reflected by the damaged region.

6. DISCUSSION

6.1 Effect of Damage on Lamb Waves

There are generally five goals for damage detection, each of which is gained with increasing difficulty and complexity. The first is the determination of the presence of damage in a specimen. The second is an estimation of the severity of the damage. The third goal is to be able to differentiate between various different types of damage. The fourth is to be able to calculate where the damage is located. The final is to estimate the dimensions of the damage. It appears that Lamb wave methods carry enough information potentially to meet all of these goals with a

strategically placed array of sensors and suitable processing codes, however the current scope of this research focuses on the first two goals.

The results from the narrow coupon tests clearly show the presence of damage in all of the specimens. Time traces were reproducible within a single specimen, although the results were not consistent across multiple specimens with identical forms of damage. This was due to the scatter and reflection of the waves from the various feature of damage which may not be identical specimen to specimen, which makes a "damage signature" difficult to define. The most obvious method to distinguish between damaged and undamaged specimens however is by regarding the wavelet decomposition plots. The control specimens retained over twice as much energy at the peak frequency as compared to all of the damaged specimens, and especially contained much more energy in the reflected waves. The loss of energy in the damaged specimens was due to reflection energy, and dispersion caused by the micro-cracks within the laminate in the excitation of high-frequency local modes.

The sandwich beam results were more difficult to interpret, due to the damping nature of the cores, which significantly reduced the voltage generated by the PZT sensors. Probably the most significant result of the present research was the "blind test." Four high density aluminum-core beam specimen were tested, one of which had a known delamination in its center, while of the remaining three specimens it was unknown which contained the circular disbond and which two were the undamaged controls. By comparing the four wavelet coefficient plots in **Figure 6**, one can easily deduce that the two control specimens are the ones with much more energy in the transmitted signals, while the third specimen (Control C) obviously has the flaw that reduces energy to a similar level to that of the known delaminated specimen. This test serves as a testament to the viability of the Lamb Wave method being able to detect damage in at least simple structures.

Similar effects of damage were observed in each of the built-up composite structure cases. In the stiffened plates, the Lamb waves were able to propagate across the stiffened region without much dispersion since they were well bonded and uniform across the specimen. By comparing the stiffened plates with and without a delamination, a reproducible signal was transmitted across each of the intact portions of the composite stiffeners while it was obvious that the signal traveling through the delaminated region was propagating at a different speed. Finally, in the composite sandwich cylinder the impacted region caused severe dispersion of the traveling Lamb wave, which in turn attenuated the received signal at each sensor further down the tube. For all of the tested specimens, all forms of damage were easily perceived by comparing the time of flight and wavelet coefficient magnitudes for the control

versus damaged signal. This result contributes to the argument that Lamb wave techniques could provide valuable information for the in-situ inspection of composite materials.

6.2 Comparison of Experimental and Analytical Results

Good correlation was found between the FE and experimental results. By comparing **Table 1** with **Table 2** a margin of error between 10-15% is found between the predicted and measured results for each of the narrow coupon specimens. The best agreement was found between the control model and the analog experiment since the representative damage in the test specimens did not correspond exactly to how they had been modeled, and often there were multiple forms of damage present in each specimen. It was difficult to compare the built-up composite structure experiments with the FE results for two reasons, firstly because the received signal was highly attenuated, and secondly because at the higher driving frequencies in the stiffer structures the Lamb waves traveled much quicker so that the response wave was received within the noise of the actuating signal (as described in the above section on parasitic capacitance). While the time of flight was difficult to compare for these structures, the trends observed in each of the models was verified by experimental results. Lamb waves propagating in sandwich structures of any core material demonstrated much lower displacement amplitudes than those traveling in thin laminates. More attenuation due to higher dispersion was observed in Lamb waves propagating in the circumferential direction of curved models and specimens. Lastly, good correlation was found between the experimental results and the FE results for the times of flight in the stiffened plate with and without delamination, with margins of error of 10% and 2% respectively. The results for Lamb wave propagation within laminates appeared to have matched well enough to be able to use a simple structural FEM to simulate the waves' interaction with damage with confidence for design purposes. For sandwich structures some of the effects were captured by the 2-D shell model, however a 3-D or plain-strain model was necessary to capture all of the effects of Lamb waves traveling at different velocities in various layers. Neither of these types of models for composite material are practical to be incorporated into a vehicle structural model, so some more investigation may have to be performed in this area in the future to design a Lamb wave system for a composite sandwich structure based on FEA.

6.3 Implementation of Lamb Wave Techniques in an SHM System

Lamb wave techniques have good potential for implementation in a SHM system. These methods provide useful information about the presence, location, type, size and extent of damage in composite materials, and can be applied to a structure with conformable piezoelectric devices. The major disadvantage of this method is that it is active; it requires a voltage supply and function generating signal to be supplied. This can be complicated in a large structure, especially if the SHM system is to be implemented wirelessly; it has been suggested in the literature however that PZT can be actuated remotely using radio frequency waves [10]. Another difficult requirement is the high data acquisition rate needed to gain useful signal resolution. If a system is sampling at 0.5 MHz from several sensors, a large volume of data will accumulate quickly; this implies the need for local processing. The data acquisition capabilities dictate the limitations of flaw size able to be resolved by a system using this method. In order to conserve power and data storage space, the Lamb wave method should most likely be placed into a SHM system in conjunction with another passive detection method, such as a frequency response method. The piezoelectric patches used to actuate the Lamb waves could passively record frequency response data until a certain threshold of change is surpassed, and then trigger the generation of Lamb waves to gain more specific data about the damaged region. Three to four piezoelectric multi-functioning actuator/sensor patches would be placed in the same vicinity in order to be able to triangulate damage location based upon reciprocal times of flight and reflected waves. Another possible scheme could rely on long strips of piezoelectric material, which would be able to send and receive large uniform Lamb waves, and integrate the received and reflected energy in order to determine the state of the material between them. The separation between sensing patches in either of these configurations would depend on several parameters such as the material properties, damping characteristics and curvature of the structure, which for flat areas could be as large as 2 meters apart [10]. The detailed specifications of the Lamb wave driving parameters to be used for a particular application would be designed by the procedure described in the optimization section.

In the previous discussion sections, it has been shown that there is a reasonable correlation between FE models and experimental results for Lamb wave propagation, so the effectiveness of this method in a particular application can be simulated easily using existing structural models with slight modifications. Lamb wave methods have demonstrated their effectiveness in detecting the presence of several forms of damage in a variety of shapes and constructions of composite components. From these experiments it has also been shown that with more research it should be possible to measure the severity, size and location of damage using these methods. For the

delaminated stiffener for example, by integrating the energy present in a series of time steps the presence of delamination should be obvious due to the non-uniform wave front, while the fringe pattern in the transmitted and reflected waves should contain enough information to determine the width of the delamination. Similarly, for the impact damaged cylinder case, a time integration of the energy transmitted would clearly reveal the damage present.

7. CONCLUSIONS

This paper has explored the optimization and application of Lamb wave methods to damage detection in composite materials. A collection of equations is offered in order to optimize the driving parameters and actuator dimensions for testing. With these tools, an optimal configuration was selected for the experimental section of this research. Using this procedure, several narrow graphite/epoxy specimens were tested with various forms of pre-existing damage, such as delamination, matrix-cracks and through–thickness holes. Similar tests were also performed on narrow sandwich beams using cores of various densities and stiffness. These tests demonstrated the feasibility of detecting several types of flaws in representative composite structures, and this method was validated successfully by a "blind test" of several beam specimens. Tests were also performed on built-up composite structures such as stiffened plates and curved sandwich structures. Analytical modeling of these specimens yielded similar results. Lamb wave techniques have the potential to provide more information than previously tested methods such as frequency response methods since they are more sensitive to the local effects of damage to a material than the global response of a structure. Similar to frequency response methods, their results are limited at higher frequencies, however their low frequency results should provide sufficient data to predict damage. The disadvantage of Lamb wave methods is that they require an active driving mechanism to propagate the waves, and the resulting data can be more complicated to interpret than for many other techniques. Overall however, Lamb wave methods have been found to be the most effective for the in-situ determination of the presence and severity of damage in composite materials of the methods examined in this research project. Future experimentation will be aimed at testing two-dimensional and built up structures using this technique, and the application of Lamb wave methods using a singe multi-purpose actuator and sensor. Structural heath monitoring systems will be an important component in future designs of air and spacecraft to increase the feasibility of their missions, and Lamb wave techniques will likely play a role in these systems.

REFERENCES

1. Hall S.R. "The Effective Management and Use of Structural Health Data." *Proceedings of the 2nd International Workshop on Structural Health Monitoring*, 1999, 265-275.
2. Kessler S.S., Spearing S.M., Atalla M.J., Cesnik CE.S. and C. Soutis. "Damage Detection in Composite Materials using Frequency Response Methods." Proceedings of the SPIE's 8th International Symposium on Smart Structures and Materials, 4-8 March 2001, Newport Beach, CA, NDE 4336-01.
3. Kessler S.S., Spearing S.M., Atalla M.J., Cesnik, C.E.S. and C. Soutis. "Structural Health Monitoring in Composite Materials using Frequency Response Methods." Accepted for publication by *Composites Part B*, June 2001.
4. Kessler S.S., Spearing, S.M. and C. Soutis. "Damage Detection in Composite Materials using Lamb Wave Methods." Proceedings of the American Society for Composites, 9-12 September 2001, Blacksburg, VA.
5. Kessler S.S., Spearing S.M. and C. Soutis. "Optimization of Lamb Wave Methods for Damage Detection in Composite Materials." Proceedings of the 3rd International Workshop on Structural Health Monitoring, 12-14 September 2001, Stanford University.
6. Kessler S.S., Spearing S.M. and C. Soutis. "Structural Health Monitoring in Composite Materials using Lamb Wave Methods." Submitted for publication to *Smart Materials and Structures*, July 2001.
7. Percival W.J. and E.A. Birt. "A Study of Lamb Wave Propagation in Carbon-Fibre Composites." *Insight: Non-Destructive Testing and Condition Monitoring*, v.39, 1997, 728-735.
8. Osmont D., Devillers D. and F. Taillade. "A Piezoelectric Based healther Monitoring System for Sandwich Plates Submitted to Damaging Impacts." *European Congress on Computational Methods in Applied Sciences and Engineering*, 2000.
9. Monkhouse R.S.C., Wilcox P.W., Lowe M.J.S., Dalton R.P. and P. Cawley. "The Rapid Monitoring of Structures using Interdigital Lamb Wave Transducers." *Smart Materials and Structures*, v.9, 2000, 304-309.
10. Valdez S.H.D. "Structural Integrity Monitoring of CFRP Laminates using Piezoelectric Devices." Ph.D. thesis, Imperial College of Science Technology and Medicine, September 2000.
11. Viktorov I.A. *Rayleigh and Lamb Waves, Physical Theory and Applications.* Plenum Press, New York, 1967.
12. Nayfeh A.H. *Wave Propagation in Layered Anisotropic Media with Applications to Composites*. v.39, Elsevier, Amsterdam, 1995.
13. Lamb H. "On Waves in an Elastic Plate." *Proceedings of the Royal Society of London. Series A, Containing Papers of a Mathematical and Physical Character*, v.93, n.651, 1917, 293-312.
14. Fripp M. "Distributed Structural Actuation and Control with Electrostrictors." SM thesis, Massachusetts Institute of Technology, June 1995.
15. Lively P. "Dynamic Structural Shape Estimation using Integral Sensor Arrays." SM thesis, Massachusetts Institute of Technology, June 2000.
16. Strang G. and T. Nguyen *Wavelets and Filter Banks.* Wellesley-Cambridge Press, Wellesley, Ma, 1996.
17. Lind R., Kyle S. and M. Brenner. "Wavelet Analysis to Characterize Non-Linearities and Predict Limit Cycles of an Aeroelastic System." *Mechanical Systems and Signal Processing*, v.15, 2001, 337-356.
18. "The Composite Materials Handbook MIL-17 Vol. 1" Guidelines for Characterization of Structural Materials." MIL-HDBK-1E, Department of Defense, 1999.
19. Dunn C. "The Analysis, Design, Manufacture, and Testing of a Composite Micro-Satellite." SM thesis, Massachusetts Institute of Technology, February 2001.
20. Anderson E.H. "Piezoceramic Induced Strain Actuation of One and Two Dimensional Structures." PhD thesis, Massachusetts Institute of Technology, June 1989.

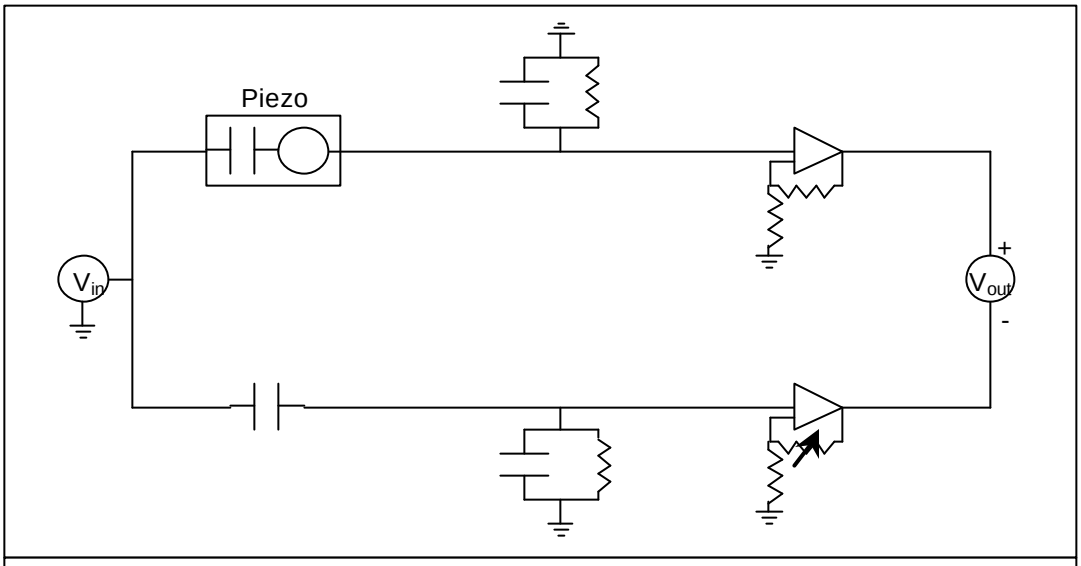

Figure 1: Self-sensing circuit allows piezoelectric actuator to sense reflected Lamb waves

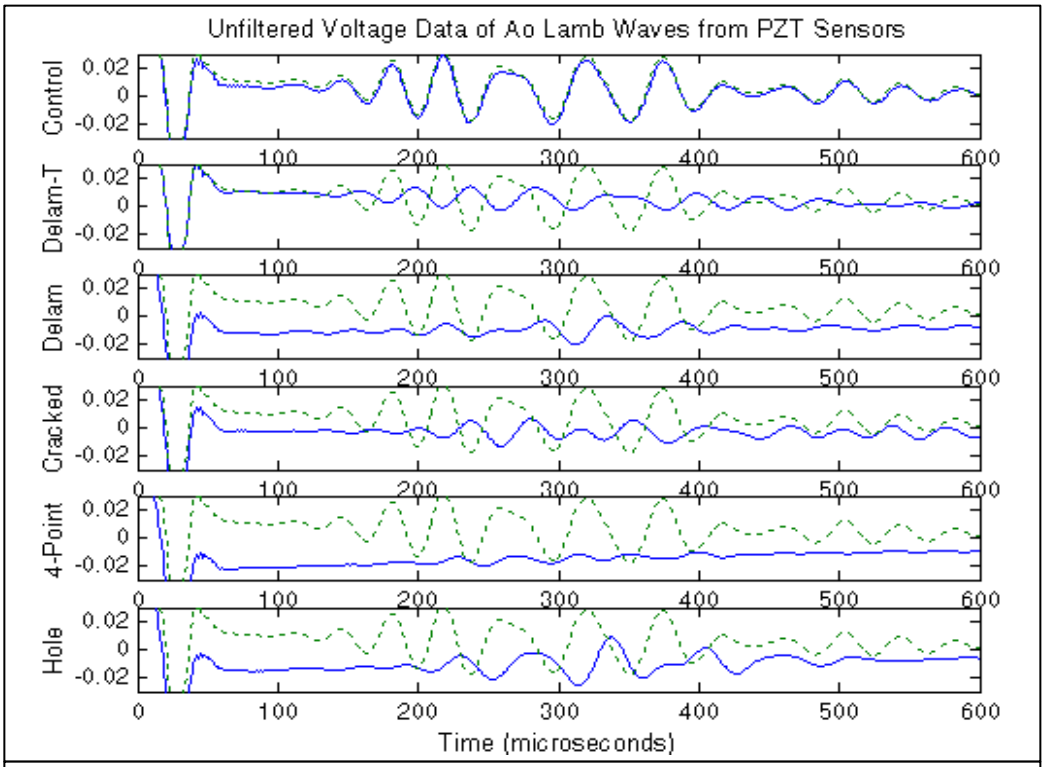

Figure 2: Time-trace of voltage signal from sensor 20 cm from actuator, 15 kHz signal
Solid lines are damaged specimens; control is superimposed as a dashed line

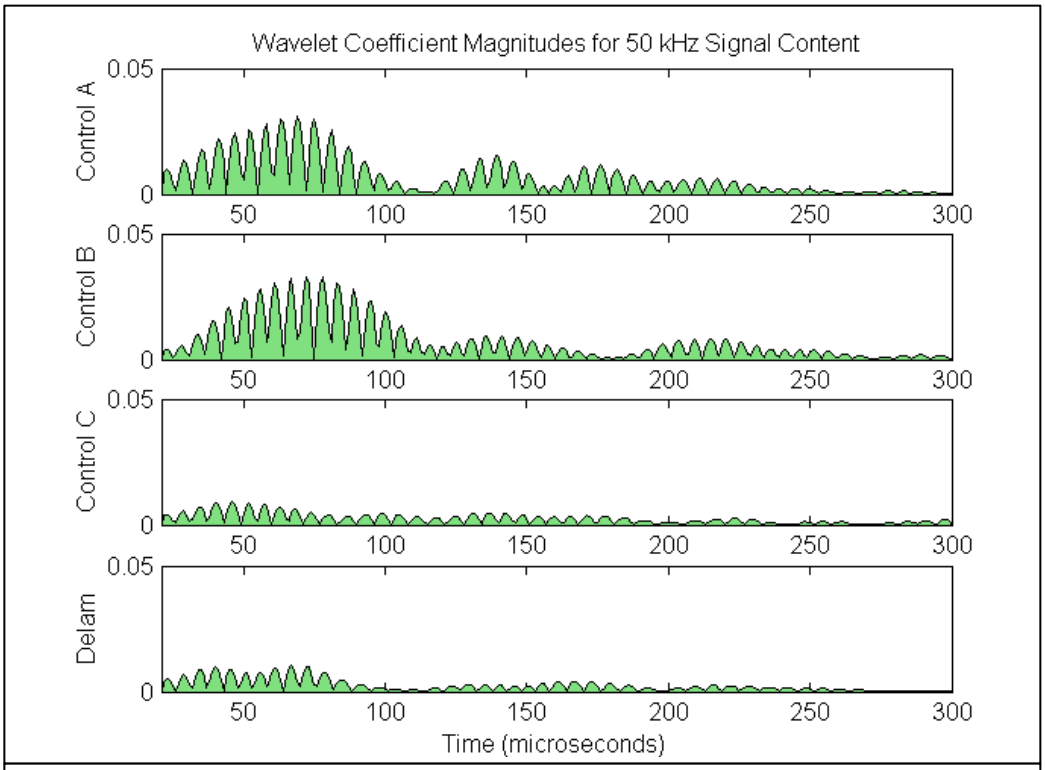

Figure 3: Wavelet coefficients for beam "blind test"; compares 50 kHz energy content

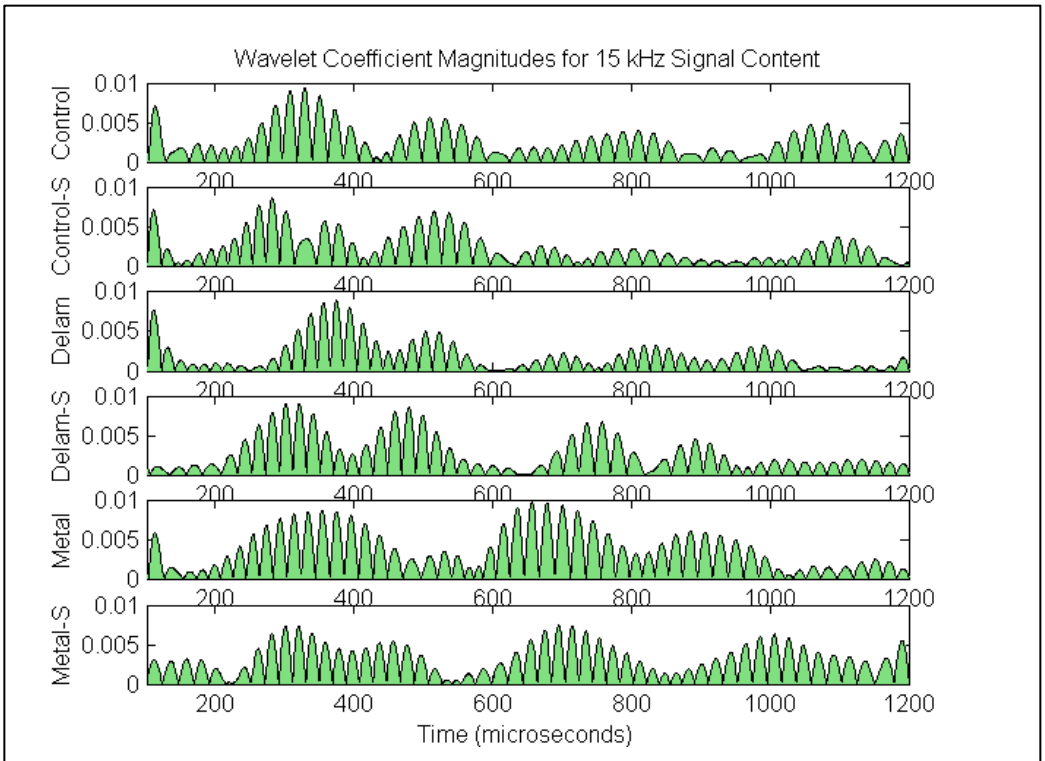

Figure 4: Wavelet coefficients for stiffened plates; compares 15 kHz energy content

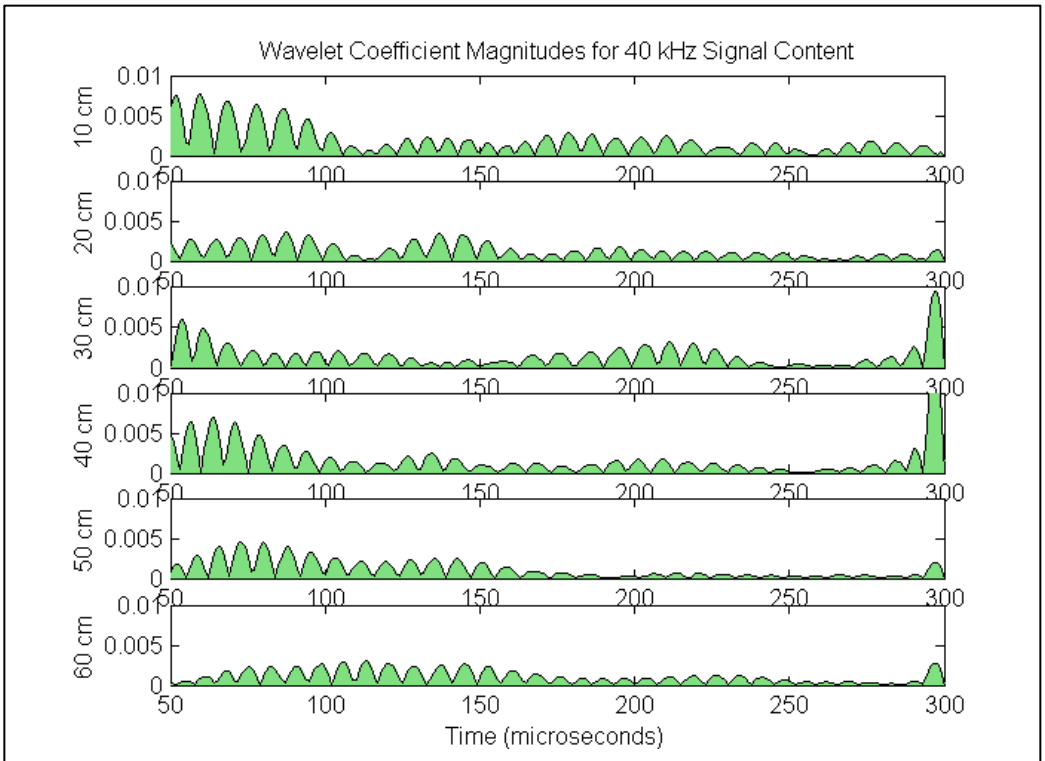

Figure 5: Wavelet coefficients for composite cylinder; compares 40 kHz energy content

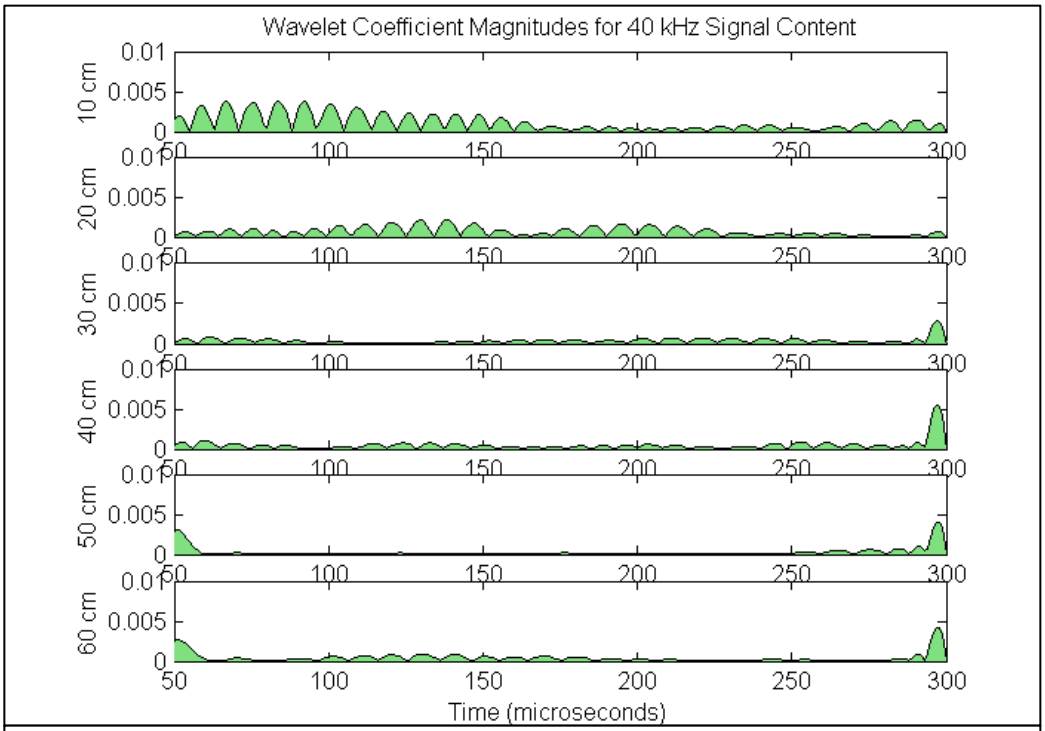

Figure 6: Wavelet coefficients for impacted cylinder; compares 40 kHz energy content

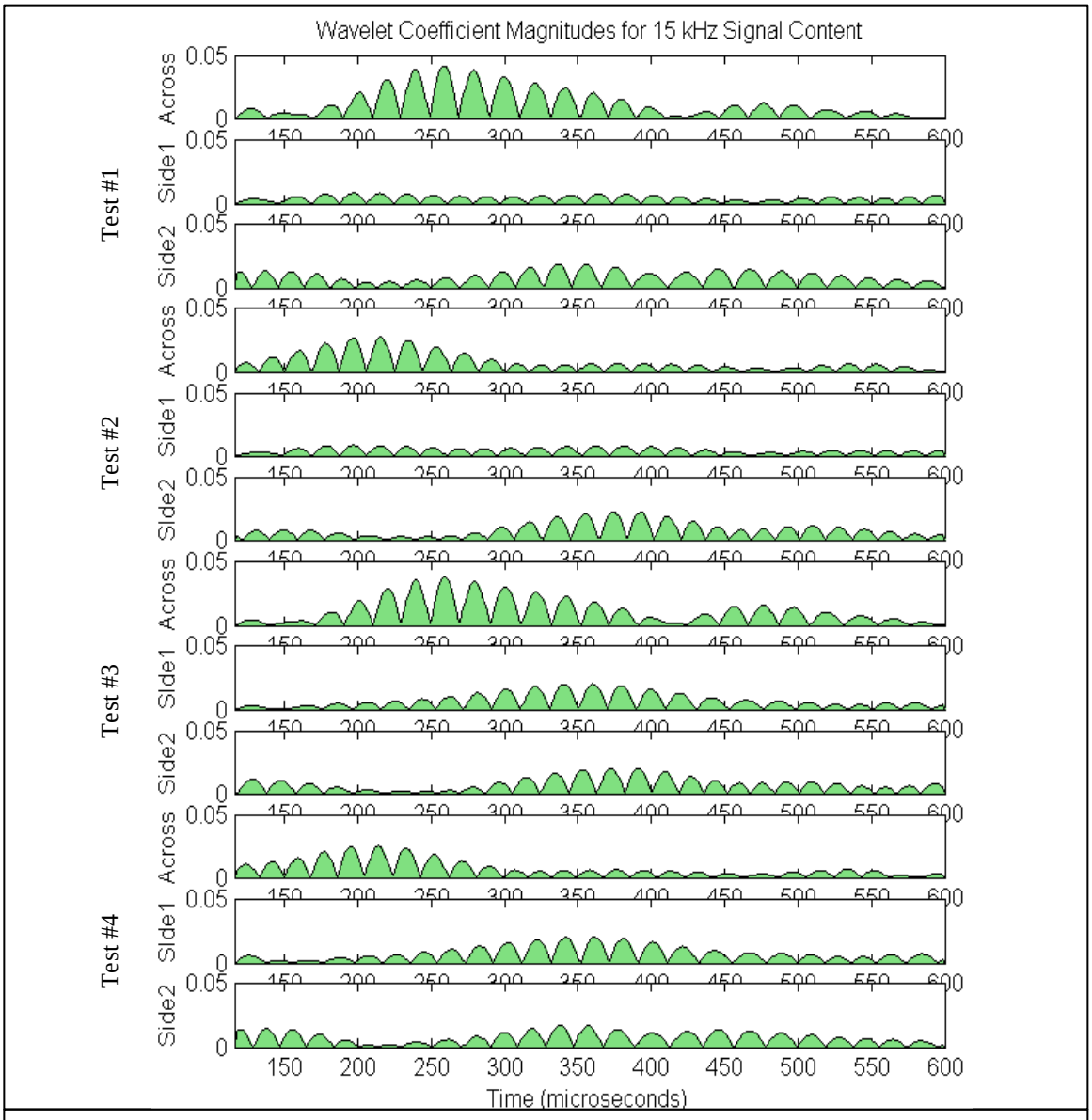

Figure 7: Wavelet coefficients for 2-D plate; compares 15 kHz energy content

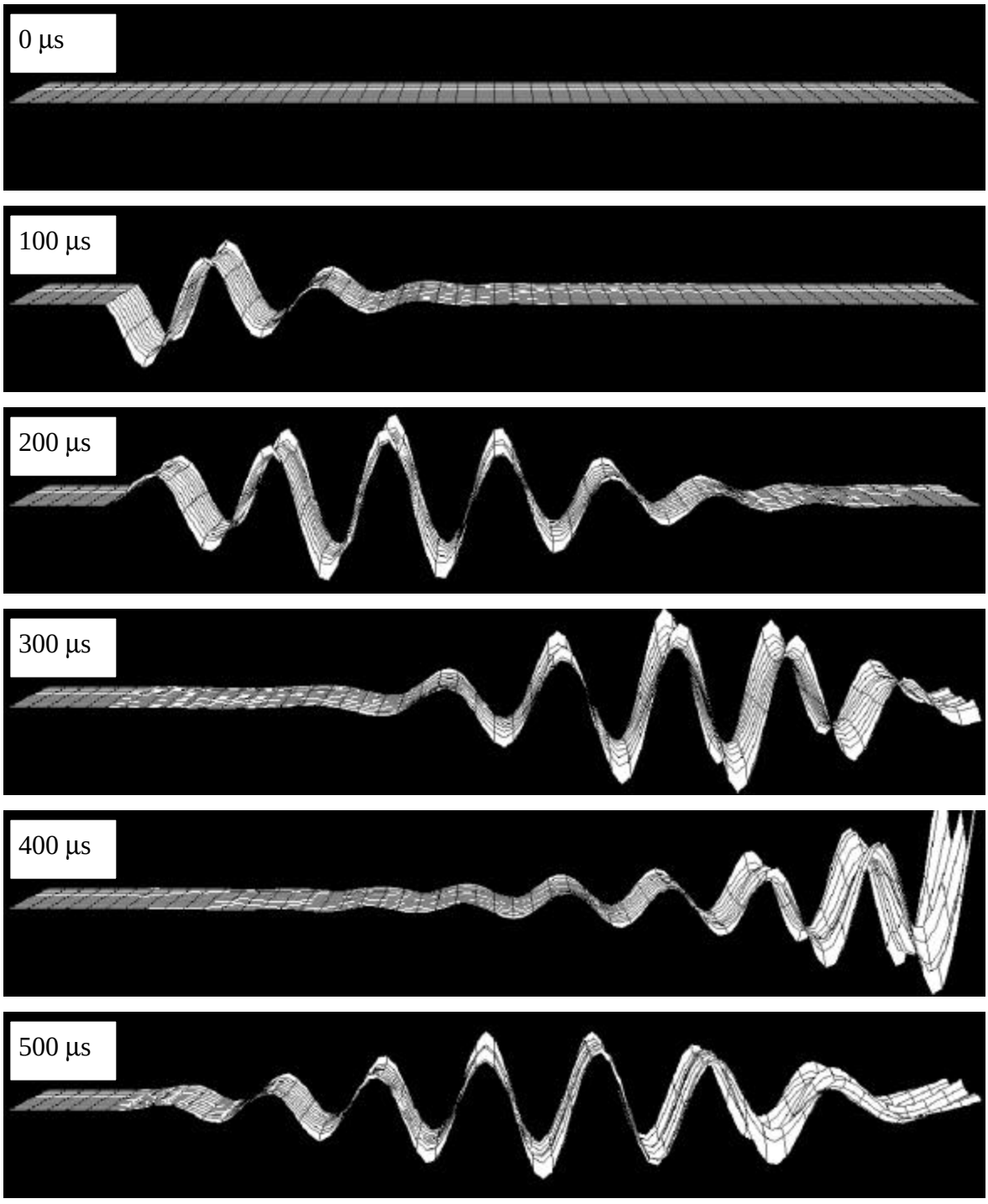

Figure 8: FEA results for narrow coupon with no damage at 100 microsecond intervals

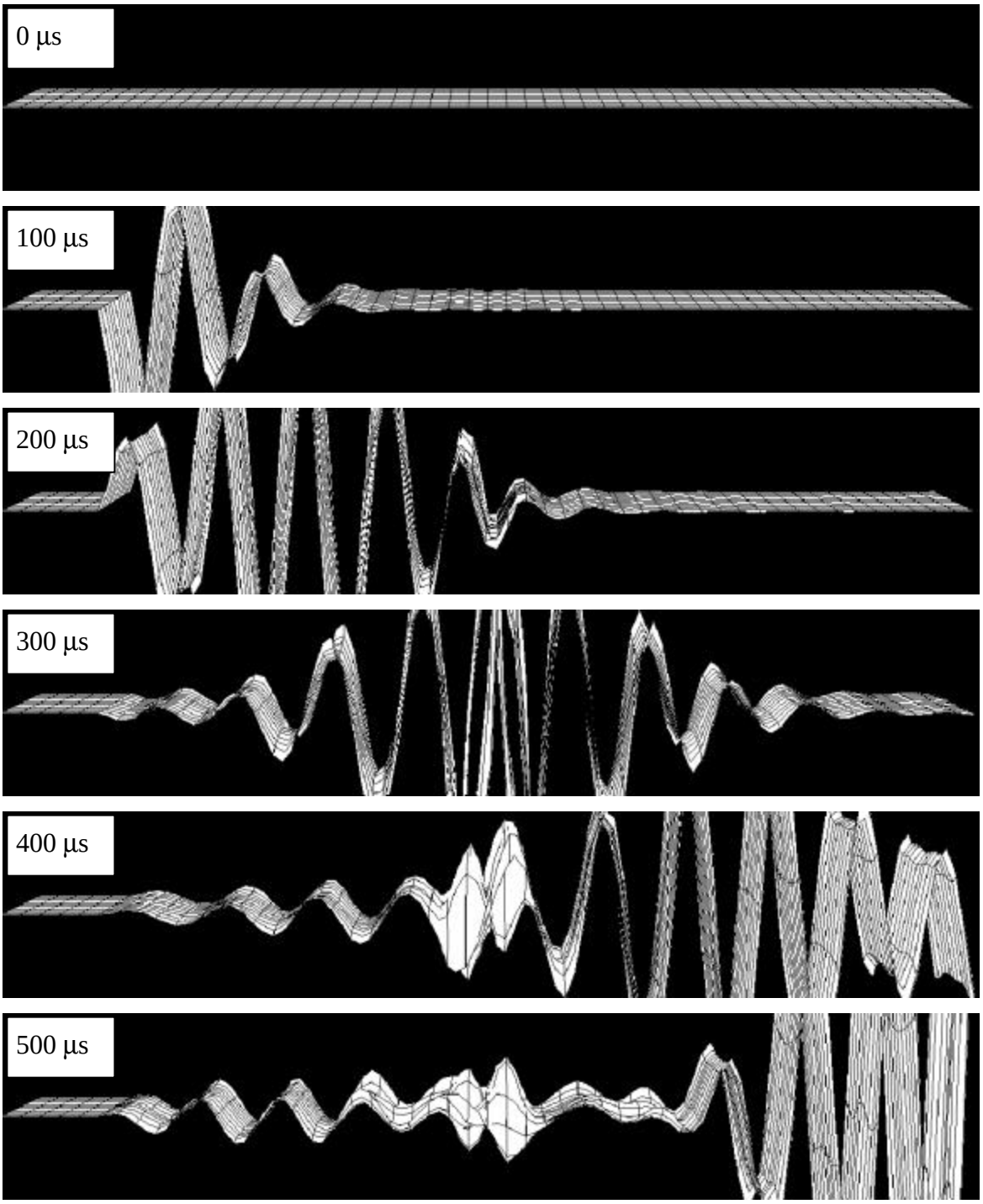

Figure 9: FEA results for narrow coupon with 25mm center delamination at 100 microsecond intervals

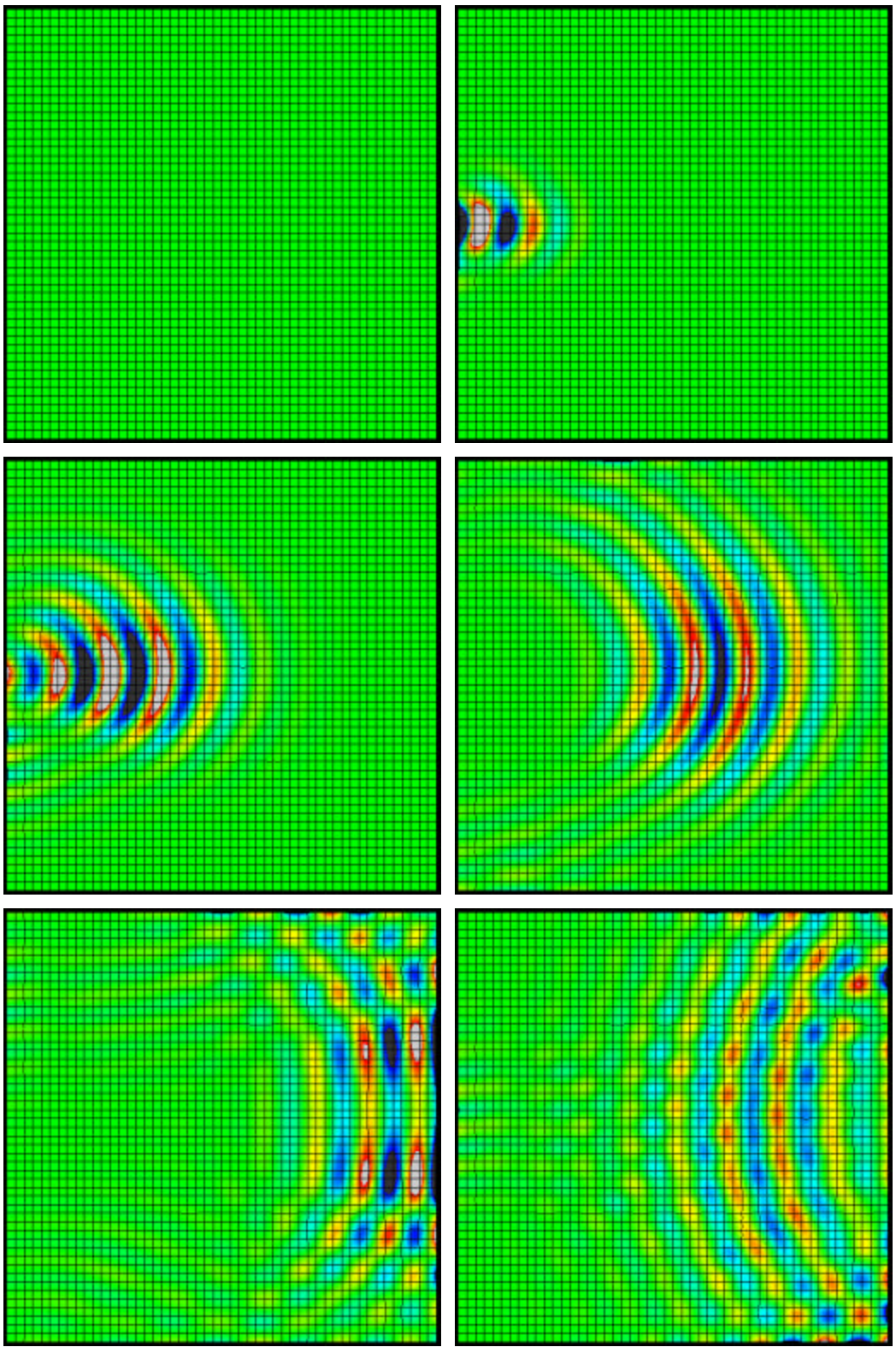

Figure 10: FEA results for 2-D plate with no stiffener at 100 microsecond intervals

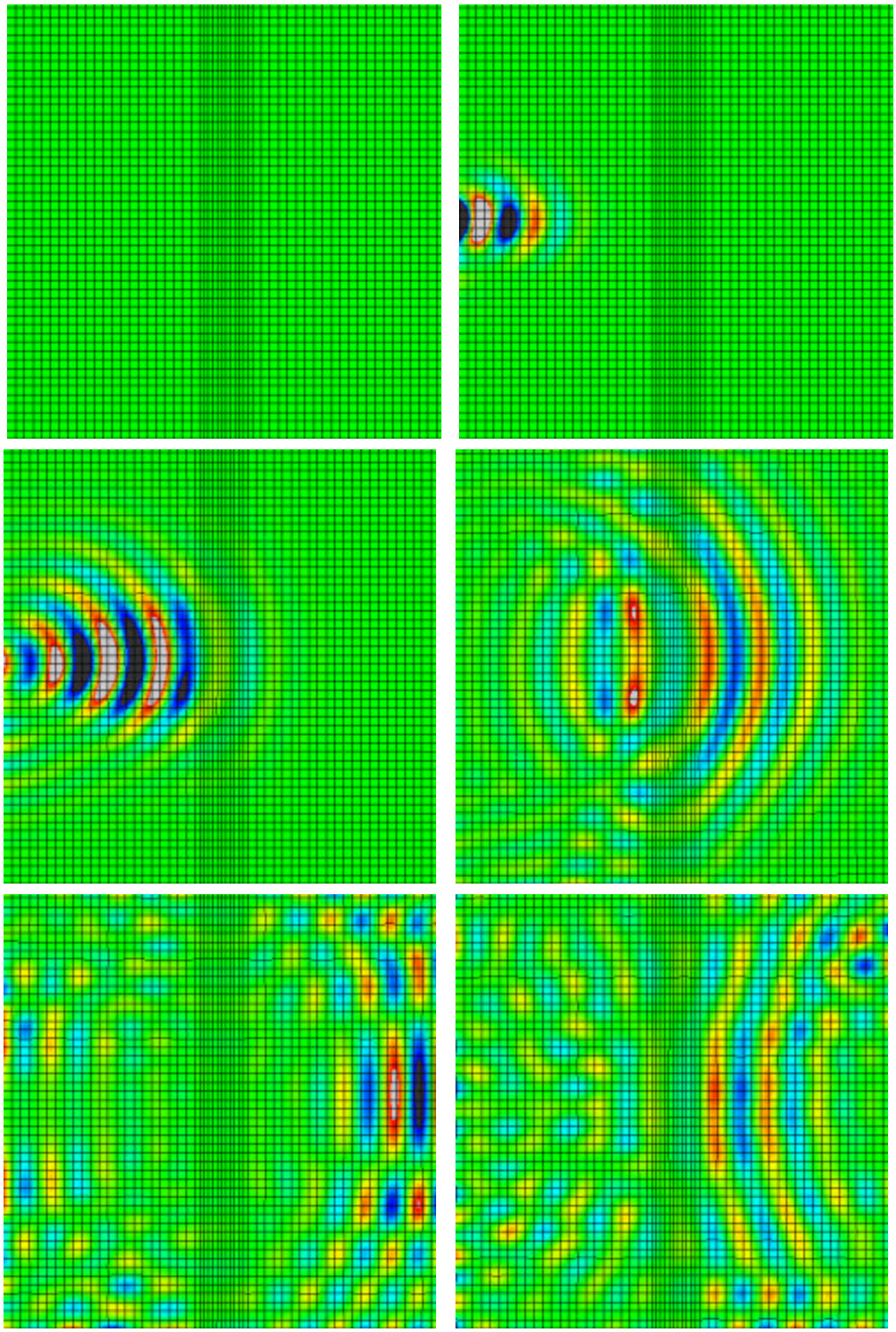

Figure11: FEA results for 2-D plate with composite stiffener (no damage) at 100 microsecond intervals

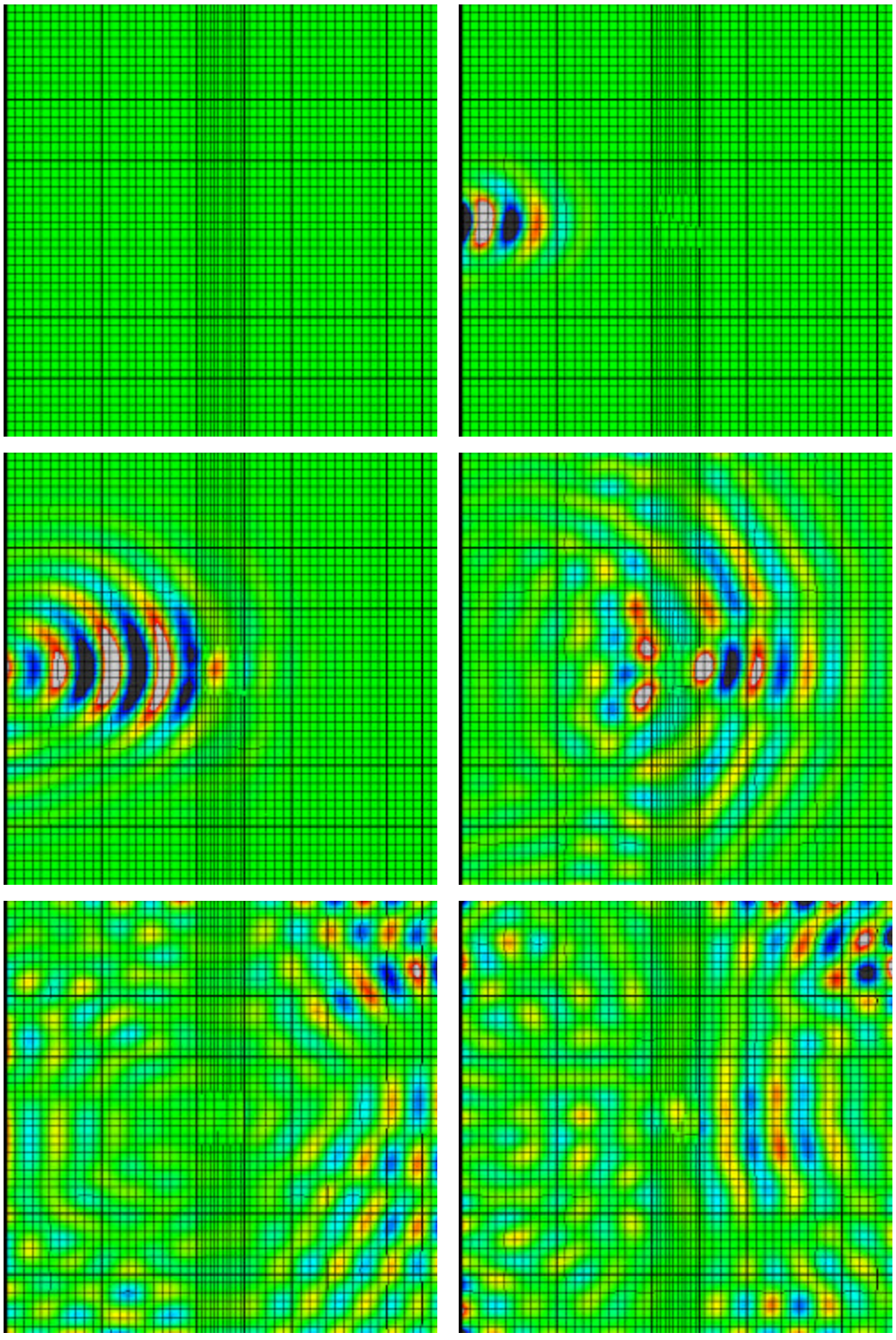

Figure 12: FEA results for 2-D plate with delaminated composite stiffener at 100 microsecond intervals

Table 1: Lamb wave times of flight and group velocities for narrow coupons as observed experimentally

(times in microseconds, velocities in m/s)	TOF based on initial arrival	TOF based on peak arrival	Cg based on initial arrival	Cg based on peak arrival	Δt from undamaged
Undamaged	216	218	952	944	-
Center cracked region	238	233	864	883	22
Center 5mm hole	226	230	910	894	10
Center 50x50mm delam	261	258	788	797	45
Side 50x25mm delam	231	220	890	935	15

Table 2: Lamb wave times of flight and group velocities for narrow coupons as observed from FEM solutions

(times in microseconds, velocities in m/s)	TOF based on initial arrival	TOF based on peak arrival	Cg based on initial arrival	Cg based on peak arrival	Δt from undamaged
Undamaged	230	230	894	894	-
Center cracked region	231	231	891	891	1
Center 5mm hole	237	231	868	891	7
Center 50x50mm delam	306	280	672	735	76
Side 50x25mm delam	292	354	704	581	62

Table 3: Lamb wave times of flight and group velocities for all geometries as observed from FEM solutions

(times in microseconds, velocities in m/s)	TOF based on initial arrival	TOF based on peak arrival	Cg based on initial arrival	Cg based on peak arrival	Δt from undamaged
High density Al	26	26	7910	7910	-
High density Al w/delam	32	36	6430	5720	6
Low density Al	45	43	4572	4780	-
2-D plate	318	290	647	709	-
2-D plate w/CFRP rib	308	310	668	664	-10
2-D plate w/CFRP rib delam	314	300	655	686	-4
2-D plate w/steel c-channel	308	290	668	709	-10